



Defect study of $\text{Cu}_2\text{ZnSn}(\text{S}_x\text{Se}_{1-x})_4$ thin film absorbers using photoluminescence and modulated surface photovoltage spectroscopy

Xianzhong Lin, Ahmed Ennaoui, Sergiu Levcenko, Thomas Dittrich, Jaison Kavalakkatt, Steffen Kretzschmar, Thomas Unold, and Martha Ch. Lux-Steiner

Citation: *Applied Physics Letters* **106**, 013903 (2015); doi: 10.1063/1.4905311

View online: <http://dx.doi.org/10.1063/1.4905311>

View Table of Contents: <http://scitation.aip.org/content/aip/journal/apl/106/1?ver=pdfcov>

Published by the AIP Publishing

Articles you may be interested in

[Interference effects in photoluminescence spectra of \$\text{Cu}_2\text{ZnSnS}_4\$ and \$\text{Cu}\(\text{In,Ga}\)\text{Se}_2\$ thin films](#)

J. Appl. Phys. **118**, 035307 (2015); 10.1063/1.4926857

[Determination of deep-level defects in \$\text{Cu}_2\text{ZnSn}\(\text{S,Se}\)_4\$ thin-films using photocapacitance method](#)

Appl. Phys. Lett. **106**, 243905 (2015); 10.1063/1.4922810

[Investigation of combinatorial coevaporated thin film \$\text{Cu}_2\text{ZnSnS}_4\$. I. Temperature effect, crystalline phases, morphology, and photoluminescence](#)

J. Appl. Phys. **115**, 173502 (2014); 10.1063/1.4871664

[Correlation between processing conditions of \$\text{Cu}_2\text{ZnSn}\(\text{S}_x\text{Se}_{1-x}\)_4\$ and modulated surface photovoltage](#)

Appl. Phys. Lett. **102**, 143903 (2013); 10.1063/1.4801463

[The role of structural properties on deep defect states in \$\text{Cu}_2\text{ZnSnS}_4\$ studied by photoluminescence spectroscopy](#)

Appl. Phys. Lett. **101**, 102102 (2012); 10.1063/1.4750249

The advertisement features a blue background with a molecular structure of spheres. On the left is a thumbnail of an 'Applied Physics Reviews' journal cover showing a 3D lattice structure. The main text reads 'NEW Special Topic Sections' in large white font. Below this, it says 'NOW ONLINE' in yellow, followed by 'Lithium Niobate Properties and Applications: Reviews of Emerging Trends' in white. The AIP Applied Physics Reviews logo is in the bottom right corner.

NEW Special Topic Sections

NOW ONLINE
Lithium Niobate Properties and Applications:
Reviews of Emerging Trends

AIP Applied Physics Reviews

Defect study of $\text{Cu}_2\text{ZnSn}(\text{S}_x\text{Se}_{1-x})_4$ thin film absorbers using photoluminescence and modulated surface photovoltage spectroscopy

Xianzhong Lin,^{a)} Ahmed Ennaoui, Sergiu Levcenko, Thomas Dittrich, Jaison Kavalakkatt, Steffen Kretzschmar, Thomas Unold, and Martha Ch. Lux-Steiner
 Helmholtz-Zentrum Berlin für Materialien und Energie, Hahn-Meitner-Platz 1, D-14109 Berlin, Germany

(Received 13 November 2014; accepted 18 December 2014; published online 5 January 2015)

Defect states in $\text{Cu}_2\text{ZnSn}(\text{S}_x\text{Se}_{1-x})_4$ thin films with $x = 0.28, 0.36,$ and 1 were studied by combining photoluminescence (PL) and modulated surface photovoltage (SPV) spectroscopy. A single broad band emission in the PL spectra was observed and can be related to quasi-donor-acceptor pair transitions. The analysis of the temperature dependent quenching of the PL band ($x = 0.28, 0.36,$ and 1) and SPV ($x = 0.28$) signals resulted in activation energies below 150 meV for PL and about 90 and 300 meV for SPV. Possible intrinsic point defects that might be associated with these observed activation energies are discussed. © 2015 AIP Publishing LLC.

[<http://dx.doi.org/10.1063/1.4905311>]

As a promising candidate as absorber layer for thin film solar cell applications, $\text{Cu}_2\text{ZnSn}(\text{S}_x\text{Se}_{1-x})_4$ (CZTSSe) based thin film solar cells have achieved efficiencies as high as 12.6% recently reported by Wang *et al.*¹ For the mass production of this material in solar energy conversion, further improvement of the solar cells performance is required. Detailed understanding of material fundamental properties such as optical and electrical properties is essential for further improvement of the solar cell performance. Defects play an important role for the doping and thus band bending as well as the recombination paths in solar cells. Therefore, understanding defect properties is crucial for the deposition of high quality absorber materials, which in turn helps to improve the solar cell performance. Generally, defects are studied by low temperature photoluminescence (PL), admittance spectroscopy, or surface photovoltage spectroscopy.

There are a few reports using PL spectroscopy to study the defect properties of CZTSSe thin films.^{2,3} However, there is no consensus in the involving recombination mechanisms. Among these reports, for the interpretation of the observed broad PL band emission quasi-donor-acceptor pair (QDAP),⁴ donor-acceptor pair (DAP),^{5–9} band-to-impurity recombination,^{2,10,11} and free-to-bound¹² were suggested. As for PL derived activation energies, values of about $30\text{--}70\text{ meV}$ for CZTS^{7–9} and CZTSe^{3,6} and deeper defects of 140 and 300 meV for CZTS^{10,12} were determined. For the PL properties of CZTSSe series, only an influence of the S/Se ratio was studied while no information on the defect involved was given.³ Previously, we have reported synthesis of CZTSSe thin films from binary and ternary chalcogenide nanoparticle precursors.^{13,14} Furthermore, we have reported the influence of annealing conditions on the surface photovoltage properties of the resulting CZTSSe thin films.¹⁵ To obtain more fundamental information about CZTSSe thin films, PL spectroscopy combined with surface photovoltage spectroscopy (SPV) was used to study the defect properties of CZTSSe thin films.

$\text{Cu}_2\text{ZnSn}(\text{S}_x\text{Se}_{1-x})_4$ thin films with $x = 0.28, 0.36,$ and 1 on molybdenum coated glass substrate were prepared by annealing Cu-Zn-Sn-S precursor thin films spin coated from ZnS, SnS, and Cu_3SnS_4 nanoparticle precursors under sulphur or selenium containing atmosphere. Detailed preparation conditions can be found in our previous publication.^{15,16} The overall chemical composition determined by energy dispersive X-ray spectroscopy are $\text{Cu}/(\text{Zn} + \text{Sn}) = 0.72, 0.93,$ and $1.0,$ and $\text{Zn}/\text{Sn} = 1.0, 1.25$ and 1.5 for $\text{Cu}_2\text{ZnSn}(\text{S}_x\text{Se}_{1-x})_4$ samples with $x = 0.28, 0.36,$ and $1.0,$ respectively. The PL measurements were performed using a diode laser with a wavelength of 660 nm as an excitation source. A set of neutral density filters was used for variation of the excitation intensities from $500\text{ mW}/\text{cm}^2$ up to $500\text{ W}/\text{cm}^2$. The samples are mounted on the cold finger of a closed-cycle helium cryostat, which allows the measurement at temperatures down to 20 K . The emission spectra were analysed by a monochromator and the signals were detected with a thermoelectrically cooled CCD or InGaAs detector.

Figure 1 shows the PL spectra of all three CZTSSe thin films measured at 20 K with 10% of the maximum diode laser power. Similar to the literature reports, only a broad peak was detected while narrow excitonic lines were not detected for these samples.^{5,7,11} The emission peaks are located at $1.00, 1.04,$ and 1.18 eV for samples with $x = 0.28, 0.36,$ and $1,$ respectively. These values are significantly smaller than the room temperature band gaps of the corresponding samples, 1.15 eV for sample with $x = 0.28, 1.28\text{ eV}$ for sample with $x = 0.36,$ and 1.55 eV for sample with $x = 1.0$. The band gaps of samples with $x = 0.28$ and 0.36 were estimated by quantum efficiency measurements which will be published elsewhere, while the band gap of sample $x = 1.0$ was determined by optical measurement.¹³ According to the studies,^{3,16–20} the band gap of CZTSSe increases with increasing sulphur content in the samples. Hence, the shift of the PL peak position is related to the chemical composition of the samples, especially the $[\text{S}]/[\text{S} + \text{Se}]$ ratios. There is no one to one agreement between PL and absorption shifts, which points to the fact that the defects involved in the PL transitions have different energy levels. Additionally, among these samples, sample with

^{a)} Author to whom correspondence should be addressed. Electronic mail: lin.xianzhong@helmholtz-berlin.de.

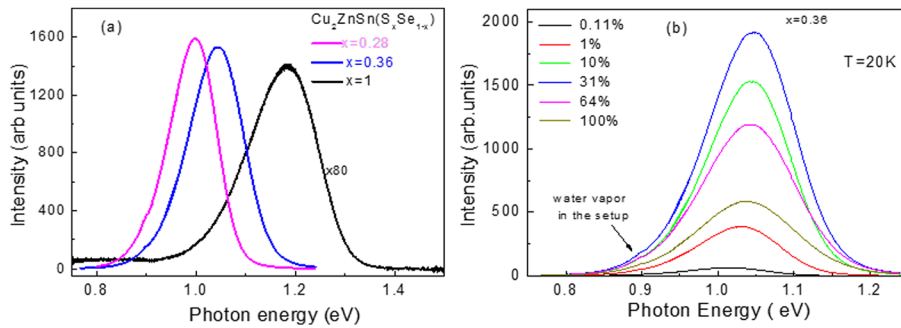


FIG. 1. (a) PL spectra of different samples measured at 20 K with an excitation power density of 50 W/cm^2 . To get a better view on the shift of the peaks, the spectrum of sample A has been multiplied by 80. (b) Typical evolutions of PL spectra with increasing excitation power for $x = 0.36$ measured at 20 K. The power excitation changed from 0.11% to 100% of the maximum excitation power density (500 W/cm^2).

lowest sulphur content shows the strongest PL signal, while the pure sulphide CZTS sample displays the weakest PL signal.

To investigate the recombination mechanisms, excitation power and temperature-dependent PL measurements were performed. Figure 1(b) shows the PL spectra of $\text{Cu}_2\text{ZnSn}(\text{S}_{0.36}\text{Se}_{0.64})_4$ sample measured with different excitation power at 20 K. The PL intensity increases with increasing excitation intensity. However, when the excitation intensity exceeded 30% of the maximum excitation intensity of 500 W/cm^2 , the PL intensity decreased with increasing excitation power. This is due to a heating effect of the laser on the sample. A similar phenomenon was also observed on $\text{Cu}_2\text{ZnSn}(\text{S}_{0.28}\text{Se}_{0.72})_4$.

Figure 2 summarizes the evolution of the PL peak positions and integrated PL intensity with increasing excitation power for all three samples. As can be seen from Figure 2(a), the integrated PL intensity increased linearly with increasing excitation power before the observation of heating effect on the samples. The slopes are determined to be 0.86, 0.71, and 0.65 for $\text{Cu}_2\text{ZnSnS}_4$, $\text{Cu}_2\text{ZnSn}(\text{S}_{0.36}\text{Se}_{0.64})_4$, and $\text{Cu}_2\text{ZnSn}(\text{S}_{0.28}\text{Se}_{0.72})_4$, by fitting the curves with a power exponent function, respectively. All these values are smaller than 1, indicating that the recombination mechanisms involved for all the samples are defect related.^{6,7,21} Figure 2(b) illustrates the evolution of the PL peak positions with increasing excitation power. The shift of the PL peak energies with increasing excitation power are 5, 14, and 11 meV/decade for $\text{Cu}_2\text{ZnSnS}_4$, $\text{Cu}_2\text{ZnSn}(\text{S}_{0.36}\text{Se}_{0.64})_4$, and $\text{Cu}_2\text{ZnSn}(\text{S}_{0.28}\text{Se}_{0.72})_4$, respectively. Blue shifts of the PL peaks with excitation intensity are a feature of DAP recombination process.^{22,23} Peak energies of DAP recombination can be expressed by equation

$$h\nu_{\max} = E_g - (E_A + E_D) + \frac{e^2}{4\pi\epsilon_0\epsilon_r r}, \quad (1)$$

where E_D and E_A are the donor and acceptor ionization energies, respectively, r is the distance between the donor and acceptor involved in the emission, e is the electron charge, ϵ denotes the static dielectric constant, and ϵ_0 is the permittivity of vacuum. However, the shift of the PL peak energies for both $\text{Cu}_2\text{ZnSn}(\text{S}_{0.36}\text{Se}_{0.64})_4$ and $\text{Cu}_2\text{ZnSn}(\text{S}_{0.28}\text{Se}_{0.72})_4$ is larger than 10 meV/decade , which might suggest that the recombination processes is not related to DAP with a shallow defect involved for which a smaller shift is typically observed.²⁴ Leitão *et al.*⁷ have observed that the PL peak suffers a blue shift at a rate of 23.5 meV/decade in CZTS thin films as the excitation power increases. Combining with the temperature dependent PL measurements and electronic characterisation, they suggested that this behavior can be explained by potential fluctuations, which might be responsible for our PL band shift under excitation, too. For the case of the potential fluctuations effects on DAP type transitions, the recombination is a quasi-DAP type.²⁵

To further understand the recombination process, temperature dependent PL measurements were carried out down to 20 K using a laser intensity of 50 W/cm^2 . Figure 3(a) illustrates the PL spectra as a function of the temperature. As the measured temperature increases, the PL signal decreases rapidly because of the increase of the active nonradioactive channels, which act as the dominate recombination process at higher temperature. Particularly, the PL signal is too small to be detected above 250 K for this sample. The same behavior is also observed for $\text{Cu}_2\text{ZnSn}(\text{S}_{0.28}\text{Se}_{0.72})_4$. Contrarily, the decline of the PL signal for sample $\text{Cu}_2\text{ZnSnS}_4$ is not as fast as for the other two samples such that the PL signal can even be detected at room temperature. Additional to the decrease of the PL signal, the PL peak energies exhibit strong dependency on temperature. The detailed evolution of the PL peak energies versus temperatures for all three samples can be found in Figure 3(b).

Figure 3(c) shows the integrated PL intensity versus the inverse temperature. The integrated PL intensities for

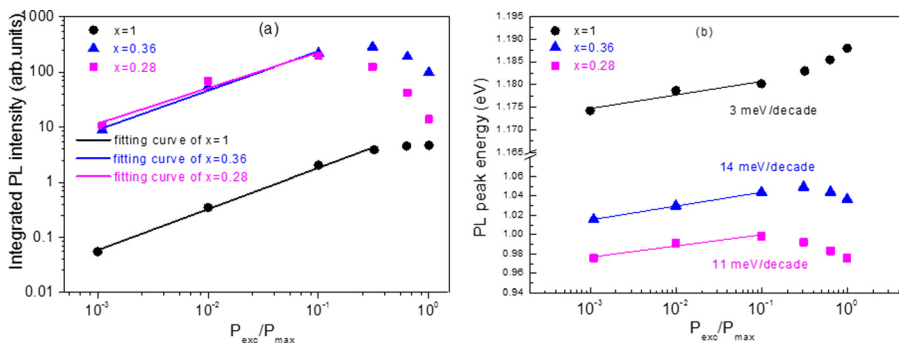


FIG. 2. Evolutions of (a) integrated PL intensities and (b) PL peak positions with increasing excitation power P for all three samples measured at 20 K.

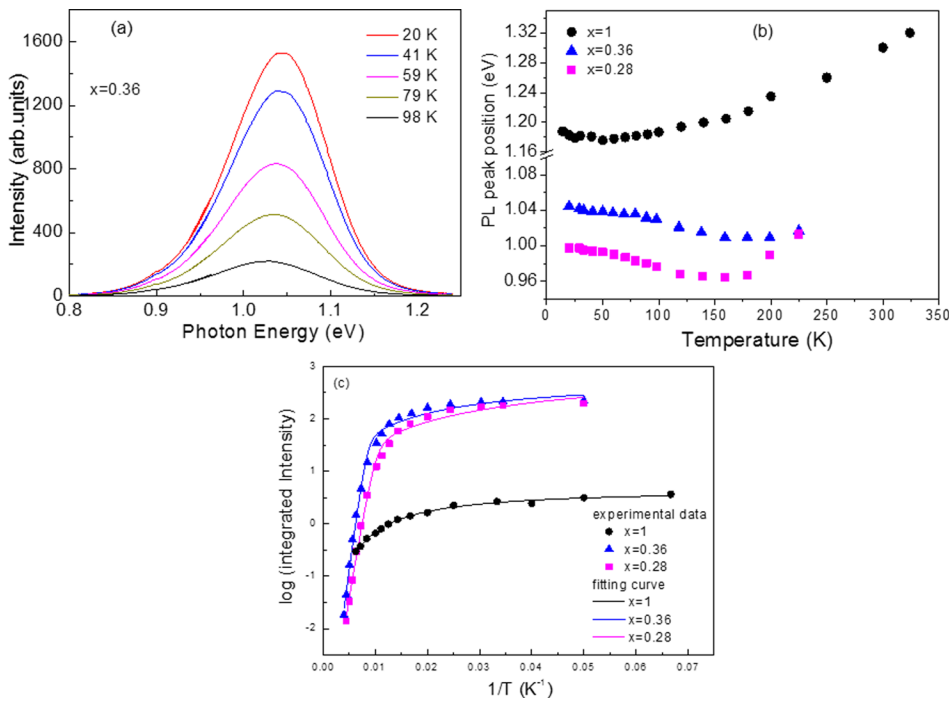


FIG. 3. (a) Typical evolutions of the PL spectra with varied temperatures for $x=0.36$ sample measured with an excitation power density of 50 W/cm^2 ; (b) the PL peak position as a function of samples temperatures for all three samples; and (c) dependence of the integrated PL intensity on temperature for 50 W/cm^2 excitation.

CZTSSe with $x=0.36$ and 0.28 suffer around 4 orders of magnitude quenching above 50 K while CZTSSe with $x=1.0$ shows slower quenching compared with selenium containing samples. To find out the activation energies involved in the recombination process, a one-activation-energy model, Eq. (2), is used to fit the Arrhenius plot²⁶

$$I(T) = \frac{I_0}{1 + C_1 T^3 + C_2 T^3 \exp\left(-\frac{E_a}{kT}\right)}, \quad (2)$$

where I_0 is the intensity extrapolated to $T=0 \text{ K}$, k is the Boltzmann constant, C_1 and C_2 are the process rate parameters, and E_a are the thermal activation energies for the involving defect states. All the fitting parameters are listed in Table I.

The activation energy for the DAP recombination process in the pure sulfide sample is found to be $20 \pm 10 \text{ meV}$, which is close to the value of 39 meV for the DAP recombination in stoichiometry CZTS reported by Miyamoto *et al.*⁹ According to the theoretical calculation reported by Chen *et al.*, the acceptor defect level of V_{Cu} is 20 meV above the valence band and the formation energy of this defect is quite low, particularly in the Cu-poor sample.²⁷ Therefore, the defect level with activation energy at $20 \pm 10 \text{ meV}$ in pure sulfide CZTS sample could be related to the V_{Cu} .

The activation energies at $121 \pm 7 \text{ meV}$ and $94 \pm 6 \text{ meV}$ were found for CZTSSe with $x=0.36$ and $x=0.28$, respectively, by fitting the Arrhenius plots with Eq. (2). Since

CZTSSe is a multinary compound, there are a lot of possible donor defects such as $(\text{Zn}_{\text{Cu}})^+$, $V_{\text{S/Se}}^{2+}$, Cu_i^+ , Zn_i^+ , and $\text{Sn}_{\text{Cu}}^{3+}$ and acceptor defects such as Cu_{Zn}^- , V_{Cu}^- , V_{Zn}^- , and V_{Sn}^- in the CZTSSe compounds. According to the theoretical calculation by Chen *et al.*,²⁷ the donor levels below 200 meV in pure sulfide CZTS include $(\text{Zn}_{\text{Cu}})^+$ (150 meV), Cu_i^+ (110 meV), and Sn_{Cu} (30 meV), while the acceptor levels below 200 meV include Cu_{Zn}^- (150 meV) and V_{Cu}^- (20 meV). All these defects show lower levels in pure selenide CZTSe sample due to the weaker hybridization effect.²⁷ Hence, the defect states observed for CZTSSe with $x=0.36$ and $x=0.28$ could be possibly attributed to either the donor levels of $(\text{Zn}_{\text{Cu}})^+$ and Cu_i^+ or the acceptor level of Cu_{Zn}^- . However, the EDX analysis, which is not shown here, reveals that both of the samples are Cu poor and Zn rich. Therefore, the presence of $(\text{Zn}_{\text{Cu}})^+$ donor should be more probable in both CZTSSe with $x=0.36$ and $x=0.28$. It should be noted that higher activation energy was found in CZTSSe with $x=0.36$ ($E_a = 121 \pm 7 \text{ meV}$) than that in CZTSSe with $x=0.28$ ($E_a = 94 \pm 6 \text{ meV}$), which is in agreement with the hybridization effect due to higher amount S in $x=0.36$ sample than that in $x=0.28$.²⁷

To further understand charge carrier recombination processes in CZTSSe samples, temperature-dependent SPV measurements were carried out on CZTSSe sample with $x=0.28$. The SPV measurements were performed in a fixed capacitor arrangement.^{15,28} The measurements were carried out between 93 and 398 K in the photon energy range of 0.9 – 1.3 eV . Figure 4(a) shows the representative temperature

TABLE I. Fitting parameters of Eq. (2) to the dependence on temperature of the integrated PL intensity for different samples.

Samples	I_0	C_1	C_2	E_a (meV)
$x=1$	4.3 ± 0.4	4.1×10^{-3}	1.1×10^{-2}	20 ± 10
$x=0.36$	498 ± 204	8.3×10^{-3}	1440	121 ± 7
$x=0.28$	749 ± 665	2.2×10^{-2}	1610	94 ± 6

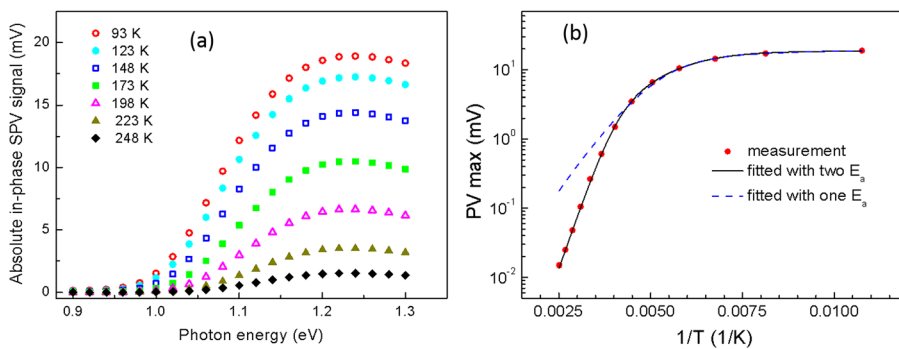


FIG. 4. (a) Temperature dependent absolute in-phase SPV spectra of CZTSSe with $x=0.28$ and (b) Temperature dependence of the maximum SPV in-phase intensity of CZTSSe with $x=0.28$ together with the fitting curve using a two activation energies model (Eq. (3)).

dependent absolute in-phase SPV spectra. The decrease of the measurement temperature leads to the increase of the absolute in-phase SPV signals. This is due to the decrease of the density of defect states, which act as recombination center of the carriers.

To find out the activation energy of the defects involving in the recombination process, a one activation energy model (Eq. (2)) was used to fit the curve, which yields an activation energy of 102 ± 12 meV. However, this fitting curve cannot cover the whole measured data points (the dashed line in Figure 4(b)). Therefore, a two activation energy model, Eq. (3), was used to fitting the experimental data, as shown in Figure 4(b)

$$I(T) = \frac{I_0}{1 + C_1 \exp\left(-\frac{E_{a1}}{kT}\right) + C_2 \exp\left(-\frac{E_{a2}}{kT}\right)}. \quad (3)$$

The two activation energies were found to be 91 ± 6 meV and 301 ± 6 meV. The activation energy of 91 ± 6 meV is very close to the value of 94 ± 6 meV determined by temperature dependent PL measurements, and might therefore also be associated with $(Zn_{Cu})^+$ defect states. Cu and Zn disorder has been revealed experimentally in kesterite type CZTS by Schorr using neutron diffraction.²⁹ On the other hand, according to calculations by Chen *et al.*,²⁷ the observed defects with the ionization energy around 300 meV could be Cu_{Sn} , Sn_{Cu} , Zn_{Sn} , V_{Zn} , V_{Sn} , or V_{Se} . Among all these defects, Cu_{Sn} and Zn_{Sn} were found to have the lowest formation energy. In particular, when the CZTSSe is Cu-poor and Zn-rich, the formation energy for Zn_{Sn} is significantly decreased and the concentration of $[Zn_{Sn} + Cu_{Zn}]$ defect states increase significantly.²⁷ Since our sample is Cu-poor and Zn rich, we proposed that Zn_{Sn} could be the observed acceptor defect.

In summary, photoluminescence properties of $Cu_2ZnSn(S_xSe_{1-x})_4$ thin films with different $S/(S+Se)$ ratios have been investigated by temperature and excitation intensity dependent measurements. The PL spectra could be attributed to a quasi-DAP recombination processes, which dominate the radiative recombination process. Defect state with activation energies at 121 ± 7 meV for $Cu_2ZnSn(S_{0.36}Se_{0.64})_4$, 94 ± 6 meV for $Cu_2ZnSn(S_{0.28}Se_{0.72})_4$, and 20 ± 10 meV for Cu_2ZnSnS_4 were observed. SPV measurement showed an activation of 91 ± 6 meV in $Cu_2ZnSn(S_{0.28}Se_{0.72})_4$, in close agreement with the PL measurement, and an additional

activation energy of 301 ± 6 meV. Possible intrinsic point defects that might be associated with these observed activation energies were discussed.

This work was carried out as part of a program supported by the BMBF (Grant No. 03SF0363B). The authors would like to thank J. Klaer for the preparation of Mo substrates. X. Z. Lin gratefully acknowledges the financial support from the China Scholarship Council, HZB, and Helmholtz Association.

- ¹W. Wang, M. T. Winkler, O. Gunawan, T. Gokmen, T. K. Todorov, Y. Zhu, and D. B. Mitzi, *Adv. Energy Mater.* **4**, 1301465 (2014).
- ²O. Gunawan, T. Gokmen, C. W. Warren, J. D. Cohen, T. K. Todorov, D. A. R. Barkhouse, S. Bag, J. Tang, B. Shin, and D. B. Mitzi, *Appl. Phys. Lett.* **100**, 253905 (2012).
- ³M. Grossberg, J. Krustok, J. Raudoja, K. Timmo, M. Altosaar, and T. Raadik, *Thin Solid Films* **519**, 7403 (2011).
- ⁴T. Gershon, B. Shin, T. Gokmen, S. Lu, N. Bojarczuk, and S. Guha, *Appl. Phys. Lett.* **103**, 193903 (2013).
- ⁵K. Tanaka, Y. Miyamoto, H. Uchiki, K. Nakazawa, and H. Araki, *Phys. Status Solidi A* **203**, 2891 (2006).
- ⁶F. Luckert, D. I. Hamilton, M. V. Yakushev, N. S. Beattie, G. Zoppi, M. Moynihan, I. Forbes, A. V. Karotki, A. V. Mudryi, M. Grossberg, J. Krustok, and R. W. Martin, *Appl. Phys. Lett.* **99**, 062104 (2011).
- ⁷J. P. Leitão, N. M. Santos, P. A. Fernandes, P. M. P. Salomé, A. F. da Cunha, J. C. González, G. M. Ribeiro, and F. M. Matinaga, *Phys. Rev. B* **84**, 024120 (2011).
- ⁸T. Tanaka, D. Kawasaki, M. Nishio, Q. Guo, and H. Ogawa, *Phys. Status Solidi C* **3**, 2844 (2006).
- ⁹Y. Miyamoto, K. Tanaka, M. Oonuki, N. Moritake, and H. Uchiki, *J. Appl. Phys.* **47**, 596 (2008).
- ¹⁰M. Grossberg, J. Krustok, J. Raudoja, and T. Raadik, *Appl. Phys. Lett.* **101**, 102102 (2012).
- ¹¹M. Grossberg, J. Krustok, K. Timmo, and M. Altosaar, *Thin Solid Films* **517**, 2489 (2009).
- ¹²S. Levchenko, V. E. Tezlevan, E. Arushanov, S. Schorr, and T. Unold, *Phys. Rev. B* **86**, 045206 (2012).
- ¹³X. Lin, J. Kavalakkatt, K. Kornhuber, S. Levchenko, M. C. Lux-Steiner, and A. Ennaoui, *Thin Solid Films* **535**, 10 (2013).
- ¹⁴J. Kavalakkatt, X. Lin, K. Kornhuber, P. Kusch, A. Ennaoui, S. Reich, and M. C. Lux-Steiner, *Thin Solid Films* **535**, 380 (2013).
- ¹⁵X. Z. Lin, T. Dittrich, S. Fengler, M. C. Lux-Steiner, and A. Ennaoui, *Appl. Phys. Lett.* **102**, 143903 (2013).
- ¹⁶X. Lin, J. Kavalakkatt, A. Ennaoui, and M. C. Lux-Steiner, *Sol. Energy Mater. Sol. Cells* **132**, 221 (2015).
- ¹⁷S. Chen, A. Walsh, J.-H. Yang, X. G. Gong, L. Sun, P.-X. Yang, J.-H. Chu, and S.-H. Wei, *Phys. Rev. B* **83**, 125201 (2011).
- ¹⁸T. K. Todorov, K. B. Reuter, and D. B. Mitzi, *Adv. Mater.* **22**, E156 (2010).
- ¹⁹J. He, L. Sun, S. Chen, Y. Chen, P. Yang, and J. Chu, *J. Alloys Compd.* **511**, 129 (2012).
- ²⁰S. C. Riha, B. A. Parkinson, and A. L. Prieto, *J. Am. Chem. Soc.* **133**, 15272 (2011).
- ²¹T. Schmidt, K. Lischka, and W. Zulehner, *Phys. Rev. B* **45**, 8989 (1992).
- ²²R. Dingle, *Phys. Rev.* **184**, 788 (1969).

- ²³D. Thomas, J. Hopfield, and W. Augustyniak, *Phys. Rev.* **140**, A202 (1965).
- ²⁴E. Zacks and A. Halperin, *Phys. Rev. B* **6**, 3072 (1972).
- ²⁵P. W. Yu, *J. Appl. Phys.* **48**, 5043 (1977).
- ²⁶J. R. Krustok, H. Collan, and K. Hjelt, *J. Appl. Phys.* **81**, 1442 (1997).
- ²⁷S. Chen, A. Walsh, X. G. Gong, and S. H. Wei, *Adv. Mater.* **25**, 1522 (2013).
- ²⁸V. Duzhko, V. Timoshenko, F. Koch, and T. Dittrich, *Phys. Rev. B* **64**, 075204 (2001).
- ²⁹S. Schorr, *Sol. Energy Mater. Sol. Cells* **95**, 1482 (2011).